Quantum Image Filtering in the Frequency Domain

Pierre Mascarade
École Normale Supérieure de Lyon
Quantum Information and Computation

29 Décembre 2016

1 Introduction

The immense computing power offered by the realisation of a quantum computer have led to an increasing interest in all branch of computer science. This computational power is mainly due to the use of three principles coming from quantum physics : quantum entanglement of states, quantum interference and quantum parallelism. When exploiting this massive parallelism, it has already be shown that in some case the quantum formulation of a complex algorithm (*Shor, Grover, Deutsch-Jozsa*) can outperform its best classical formulation. This is of interest for signal processing, where there is a need for very high performance computing to achieve real time processing, and some signal processing problems that seems unoptimizable nowadays and untracktable even for the world's largest suppercomputer, could be approach on a quantum computer.
The remarkable property of quantum information and computation have thus led to a variety of formulation and studies in the quantum setting of classical algorithm from all filed of computer science, including signal and image processing. As we will see, exploiting the remarkable properties of quantum systems remains a challenging task due to fundamentals differences between the allowed operating modes of quantum and classical machines.

We will focus on this report on the quantum image processing formalism and after some general formulation of the filed we will mainly present the work of **Simona Caraiman** and Vasile I. Mana : *Quantum Image Filtering in the Frequency Domain*, 2013. We will also need to introduce at some point the work of **Lomont** : *Quantum convolution and correlation algorithm are physically impossible*, 2003.
Quantum signal processing field is still in an early stage, and thus is confronting with fundamental aspect of its formalism, such as how to represent and store an image quantumly,

how to implement fundamental geometric operation that are used as building blocks of almost all image processing algorithm. In their paper the authors focused on one of those fundamental image processing task : *image filtering*. We will see that it's a good example of a non-trivial (and non-direct) translation to the quantum world due to the drastic differences between allowed computations in classical and quantum algorithms. We will also show that as in almost any others *many-qubits quantum system* the principle of quantum entanglement will be a valuable resource and play a key role in our algorithm formulation.

We have tried to make this report as self-sufficient as possible, bringing all the pieces needed to understand the overall problem of quantum image filtering.

2 Quantum Image representation

Multiple approachs have been proposed to represent image using a quantum computer, inspired by the images representation of image in classical computers, that captures the information about colors and their corresponding position, these approachs could be summarized in two main classes.

2.1 Single qubit color encoding

In order to itegrates information about an image into a quantum state one can uses a quantum register prepared in the state :

$$|Q\rangle = |C\rangle \otimes |P\rangle_{2n} \tag{1}$$

Pixel positions are encoded using $2n$ qubits in register $|P\rangle$ considering that we are storing an image with $N = 2^n x 2^n$ pixels. Color information is encoded in the state of a single qubit, as suggested in [6] :

$$|I(\theta)\rangle = \frac{1}{2^n} \sum_{i=0}^{2^{2n}-1} (\cos\theta_i |0\rangle + sin\theta_i |1\rangle) \otimes |i\rangle \tag{2}$$

$$\theta_i \in \left[0, \frac{\pi}{2}\right], i = 0, 1, \ldots, 2^{2n} - 1, \tag{3}$$

where $|0\rangle$, $|1\rangle$ are 2-D computational basis states, $|i\rangle$ are 2^{2n}-D computational basis states that encode the pixel position corresponding to a given color and $\theta_i = (\theta_0, \theta_1, \ldots, \theta_{2^{2n}-1})$ is a vector of angles encoding the colors.
This approach relies on the definition of a machine capable of detecting the frequency of the monochromatic electromagnetic wave that determines the color, and by establishing a

bijective relationship between these frequencies and the angle parameter of a qubit, meaning that the color information is encoded in the propability amplitudes of the corresponding one qubit state.
Despite of the efficient color encoding (1 qubits) there are several drawbacks that limit the usability of this quantum image class :

1. The classical image cannot be accurately retrieved, according to the postulate of quantum mechanics that states that the probability amplitudes of a quantum state cannot be accurately determined using a finite number of measurements. The retrieval protocol requires here too that that several instance of the input image be prepared and then a ***statistical*** protocol that aims to minimize the uncertainty of the retrieval process by *estimating* the amplitude of the quantum states encoding the colors for each pixel within a given accuracy, should be run for each image instances. The main criticism we could made about this encoding is that in addition of the fact that it has to deal with several copies of the input image, the retrieval is probabilistic.

2. Moreover there are practical limitations, on the number of colors/positions that can be physically represented using the angle parameter of the qubit due to the fact that energy separation between the state should be greater than the thermal energy. The authors state in [5], that it's not physically feasible to encode separated information in 2^{24} angles of a single qubit even if we could prepare the image with high frequencies radiation at very low temperature, this drastically limit the size of the image we can deal with, recalling that the position register $|P\rangle$ encode pixel position using $2n$ qubits (e.g a 224 a $4,096$ x $4,096$ image requires already the 2^{24} values to be encoded in the qubit angles).

3. Also this encoding doesn't allow for complex color based processing, indeed it is difficult to construct quantum algorithm based on the separation of pixels with different colors (e.g Histogram segmentation [5]) since there is a unique qubits that encode the colors for each pixel (no tensor product state).

2.2 Multiple qubits color encoding

The second class of quantum image representation, proposed by Caraiman and Manta in [4], is defined as follows :

$$Q = |C\rangle_m \otimes |P\rangle_{2n} = \frac{1}{2^n} \sum_{i=0}^{2^{2n}-1} \sum_{j=0}^{2^m-1} \alpha_{ij} |j\rangle |i\rangle \tag{4}$$

where Q is an $(m+2n)$ qubits register prepared in a state that encode both color and position of a pixel as introduce in [4]. Colors are encoded in the basis states of a sequence of qubits in register $|C\rangle$ - using $m = \log_2 L$ qubits encoding the L colors (gray levels here) composing the image - by means of a superposition of all possible colors for each pixels. Unlike in the classical case, a considerable advantage here is that the same m qubits are used to store the color of all the pixels in the image, hence only $m = 2^n$ qubits are needed to store a 2^nx2^n image composed of L gray levels, that is an an overall ***exponentially*** lower memory space usage compared to the classical case where $m2^{2n}$ bits are necessary to store the same image. This is achieved due to the principle of quantum superposition of states. The general form of the color register for a pixel $|i\rangle$ is therefore :

$$|C_i\rangle = \sum_{j=0}^{2^m-1} \alpha_{ij} |j\rangle \tag{5}$$

meaning that color information is represented using the coefficients α_{ij} where $\sum_{j=0}^{2^m-1} |\alpha_{ij}|^2 = 1,\ \forall i \in [0, 2^{2n}[$ and where $\alpha_{ij} = 1$ if the color of the i pixel is j and 0 otherwise.

Pixel positions are encoded using $2n$ qubits in register $|P\rangle$ considering that we are storing an image with $N = 2^n$x2^n pixels. Moreover register $|P\rangle$ is of the form $|y\rangle|x\rangle$, where y and x encode the row and column position of a pixel respectively.

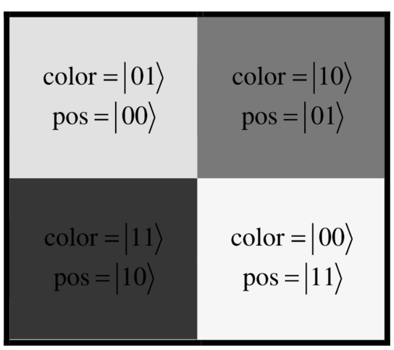

$$|Q\rangle = \frac{1}{\sqrt{2^2}} \sum_{i=0}^{2^2-1} \sum_{j=0}^{2^2-1} \alpha_{ij} |j\rangle|i\rangle =$$

$$= \frac{1}{\sqrt{2^2}} (|01\rangle|00\rangle + |10\rangle|01\rangle + |11\rangle|10\rangle + |00\rangle|11\rangle)$$

$$\alpha_{00} = 0,\ \alpha_{01} = 1,\ \alpha_{02} = 0,\ \alpha_{03} = 0$$
$$\alpha_{10} = 0,\ \alpha_{11} = 0,\ \alpha_{12} = 1,\ \alpha_{13} = 0$$
$$\alpha_{20} = 0,\ \alpha_{21} = 0,\ \alpha_{22} = 0,\ \alpha_{23} = 1$$
$$\alpha_{30} = 1,\ \alpha_{31} = 0,\ \alpha_{32} = 0,\ \alpha_{33} = 0$$

FIGURE 1 – Example of a simple 2 x 2 quantum image with four possible colors represented (2 qubits are used to represent the color information and 2 other qubits encode the pixel position

Using m qubits register basically overcome almost all the limitations stated for the *Single qubit representation* thanks to its basis states encoding of colors :

1. Allows for a ***deterministic*** retrieval of both color and pixel positions through a finite number of projective measurement, measuring the color register for a given pixel position outputs the pixel color of that pixel with unit probability
2. The number of colors that can be represented does not depend on the actual physical implementation (e.g, $m = 24$ qubits are necessary to represent the color informations of a in a 24 bits true color image, irrespective of the technology for implementing the qubit). See [5] for the complete deterministic retrieval procedure.
3. More complex image processing algorithms can be applied, since the colors are represented using a computational basis state, and can therefore act as control for some value-dependent color transform.
4. Also unlike the image representation using a lattice of qubits proposed in [7] and [6], the superposition defined in Eq. (4) allows for a simultaneous application of color operation on all pixels.

From that we think it is *the way to go* for designing complex quantum image processing algorithms, and it's the one (chosen by the authors) that we will use in the rest of this report.

2.2.1 Preparation of the quantum state representing the image

In [5] the authors showed that a quantum state representing the input image can be prepared in a two steps process.

1. First step concern the position information for all the pixels in the image stored, the superposition of the pixels position in the image is produce by applying an *Hadamard gate* on each position qubits.
2. Second step is about setting the color value for every pixel position, the color of each of the 2^{2n} pixel can be set using a $2n$-CNOTgate on each of each color qubit. Thus setting the color $|C_i\rangle$ of a pixel i as in Eq.(5), is done by inverting each qubits corresponding to a bit of 1 in the classical binary representation of C_i, and hence the qubits corresponding to a bit of 0 in the binary representation of C_i are left unchanged. The color preparation requires a sequence of at most $m2n$-CNOT gates ; this maximum boundary of gates is required when the pixel gray level color to encode is the maximum one $2^m - 1$, corresponding to the white color.

The complete preparation process can be achieved using no more than $O(mn2^{2n})$ for a 2^nx2^n image with gray level 2^m. Despite it uses more qubits, the authors have shown in

[5] that the complexity of the image preparation process is lower in their many-qubits representation than in the single-qubit representation, since the representation of the color in a single-qubit requires the use of $2^{2n} 2n$-controlled rotation gates which are expensive to compute using simple quantum gate operations.

The preparation of the quantum image in Fig.1 can be achieved using the following circuit :

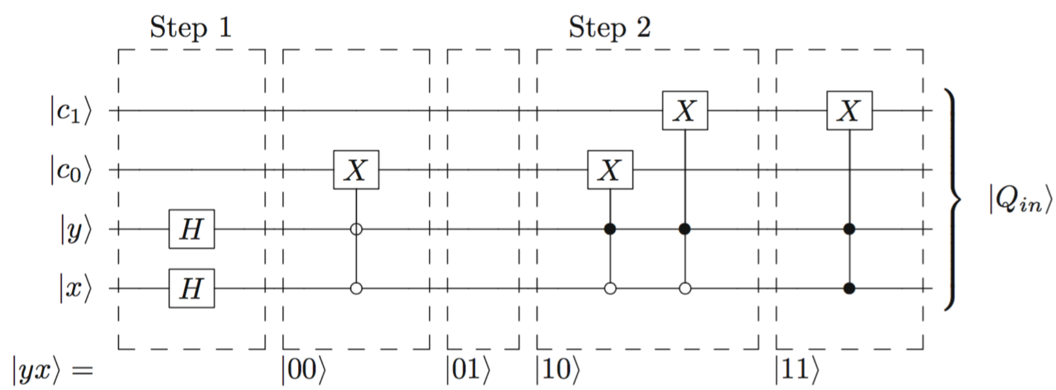

FIGURE 2 – Two steps quantum circuit for the preparation of a quantum image, where two qubits are used to encode the pixel position ($|x\rangle$ and $|y\rangle$) and two more qubit are used to encode corresponding the gray level of each pixels ($|C_0\rangle$ and $|C_1\rangle$).

3 Quantum Image Filtering in the Frequency Domain

3.1 Classical algorithm for image filtering

In classical image processing, image filtering is achieved by convolving the input image with a filter kernel, either in the spatial or in the frequency domain. For computational complexity purposes the latter is often preferred, which turns out to be a simple multiplication in the frequency domain thanks to the well known *convolution theorem* (see *Appendix* for a complete demonstration of this theorem). As one can show the frequency domain convolution become faster as the filter kernel size increases.
The classical algorithm for image filtering can be summarized in the following steps :

Algorithm 1 Classical Image Filtering

Require: $f(m,n)$, $h(m,n)$ are respectively the *input image* and the *filter kernel*
Ensure: $\hat{f}(m,n)$ is the filtered image

1: **function** IMAGE FILTERING($f(m,n)$, $h(m,n)$)
2: Compute $\mathcal{F}(u,v)$ the *Fourier Transform* of the input image $f(m,n)$
3: Compute $\mathcal{H}(u,v)$ the *Fourier Transform* of the filter kernel $h(m,n)$
4: Compute the filtered image spectrum $\hat{\mathcal{F}}(u,v) = \mathcal{F}(u,v) \cdot \mathcal{H}(u,v)$
5: Compute $\hat{f}(m,n)$ the *Inverse Fourier Transform* of $\hat{\mathcal{F}}(u,v)$
6: **return** $\hat{f}(m,n)$

with :

$$\mathcal{F}(u,v) = \sum_{m=0}^{M-1} \sum_{n=0}^{N-1} f(m,n) \cdot e^{-2i\pi\left(\frac{um}{M}+\frac{vn}{N}\right)} \tag{6}$$

$$\mathcal{H}(u,v) = \sum_{m=0}^{M-1} \sum_{n=0}^{N-1} h(m,n) \cdot e^{-2i\pi\left(\frac{um}{M}+\frac{vn}{N}\right)} \tag{7}$$

$$\hat{f}(m,n) = \frac{1}{MN} \sum_{u=0}^{M-1} \sum_{v=0}^{N-1} \hat{\mathcal{F}}(u,v) \cdot e^{+2i\pi\left(\frac{um}{M}+\frac{vn}{N}\right)} \tag{8}$$

for $u = 0,1,\ldots,M-1,\ v = 0,1,\ldots,N-1$ in (2) and (3) and $m = 0,1,\ldots,M-1,\ n = 0,1,\ldots,N-1$ in (4) where u and v are spatial frequencies, and $M = N$ for square image of size NxN. $\mathcal{F}(u,v)$ and $\mathcal{H}(u,v)$ are complex in general.

3.2 Quantum Fourier Transform and its Inverse

The Quantum Fourier Transform (QFT) on an orthonormal basis $|0\rangle, |1\rangle, \ldots, |N-1\rangle$, is the classical discrete Fourier transform applied to the vector of amplitudes of a quantum state. QFT is the unitary map defined on basis state $|x\rangle$ as :

$$|x\rangle \xrightarrow{QFT_N} \frac{1}{\sqrt{N}} \sum_{k=0}^{N-1} e^{2i\pi xk/N} |k\rangle \tag{9}$$

From the unitary of the QFT it follows that the Inverse Quantum Fourier Transform (QFT^{-1}) is defined as the Hermitian adjoint of the QFT operator : $QFT^{-1} = QFT^{\dagger}$:

$$|x\rangle \xrightarrow{QFT_N^{-1}} \frac{1}{\sqrt{N}} \sum_{k=0}^{N-1} e^{-2i\pi xk/N} |k\rangle \tag{10}$$

The QFT can be implemented on a quantum computer using Hadamard gates and Controlled-phase gates, see [3] for the proof. One can show that it can be done on quantum state of $N = 2^n$ complex values with complexity $O(\log^2 N) = O(n^2)$, that is exponentially faster than its classical counterpart (*FFT : Fast Fourier Transform*) which require $O(NlogN) = O(n2^n)$ gates for computing the Discrete Fourier Transform on 2^n elements. Even if the QFT is more efficient than its classical analogue it cannot allows using this algorithm as a direct replacement of the FFT because all Fourier coefficient in (5) are encoded in the amplitudes of a quantum state, and we know that such amplitudes cannot be directly accessed by measurements. However more subtle uses of the QFT allow exponential speed up on several classical algorithms : Shor and Grover algorithms.
Since the QFT and QFT^{-1} are implementable efficiently on a quantum computer and the FFT and FFT^{-1} (inverse FFT) are the cornerstone of the convolution algorithm, one can attempt to build a quantum analogue of the convolution algorithm that will outperform its classical counterpart. But as we are going to discuss now *the convolution algorithm is not physically realizable on a quantum computer.*

3.3 Quantum convolution algorithm is physically impossible

3.3.1 Problem Statement

Since the Fourier Tranform and the Inverse Fourier transform have their quantum counterpart, that tunrs out to be more efficient, and ar the basic building block of the convolution algorithm, one can reasonably attempt for a quantum convolution algorithm that will outperform its classical analogue. This turns out to be false and it has been shown by Lomont in [2] that that *there is no physically realisable method to compute the normalized convolution or correlation of the coefficients of two quantum states*, meaning that the precise definition of quantum convolution and quantum correlation cannot be computed without violating quantum mechanics. Let's review briefly some statement aspect of this proof. First let's defined convolution.
The ***convolution*** of two sequence of N complex numbers $S_1 = (\alpha_0, \alpha_1, \ldots, \alpha_{N-1})$ and $S_2 = (\beta_0, \beta_1, \ldots, \beta_{N-1})$ is defined to be the sequence $S_3 = (\gamma_0, \gamma_1, \ldots, \gamma_{N-1})$ given by :

$$\gamma_k = \sum_{j=0}^{N-1} \alpha_j \beta k - j \text{ for } k = 0, 1, \ldots, N-1 \tag{11}$$

where subscript are taken $mod(N)$.
The **quantum convolution problem** is stated as follows : *Given quantum states representing the two initial sequences, compute a quantum state representing the convolution*

sequence ? That is given the two states $(forN = 2^n)$

$$|\alpha\rangle = \sum_{i=0}^{N-1} \alpha_i |i\rangle \tag{12}$$

$$|\beta\rangle = \sum_{j=0}^{N-1} \beta_j |j\rangle \tag{13}$$

compute the state :

$$|\gamma\rangle = \sum_{k=0}^{N-1} \gamma_k |k\rangle \tag{14}$$

where $|\gamma\rangle$ is the normalization of the sequence given by

$$c_k = \sum_{j=0}^{N-1} \alpha_j \beta k - j \text{ for } k = 0, 1, \ldots, N-1 \tag{15}$$

Then the main theorem that claim the the convolution problem formulated as above cannot be computed by any device obeying quantum mechanics is stated as follow :
Impossibility of quantum convolution theorem : *There is no physically realisable process P to compute the (normalized) coefficients of two quantum states. That is, for arbitrary quantum states* $\sum_i a_i |i\rangle$ *and* $\sum_j b_i |b\rangle$*, there is no physically realizable process P to compute the state* :

$$\sum_{i,j=0}^{N-1} a_i b_j |ij\rangle \xrightarrow{P} \lambda \sum_{k=0}^{N-1} \sum_{j=0}^{N-1} \alpha_j \beta k - j |k\rangle \tag{16}$$

where $\lambda = 1/\sqrt{\sum_{i,j} |a_i b_j|^2}$ is the normalization factor, $N = 2^n$ for some positive integer $n > 0$. And by physically realizable process on a quantum computer, Lomont means the more general definition one can expect :
A mapping P of quantum states :

$$|\Phi\rangle \xrightarrow{P} |\Psi\rangle \tag{17}$$

is called ***physically realizable*** *if there exists a finite fixed sequence of unitary transformation and measurement operators and a quantum state* $|\rho\rangle$ *(which are extra states called "ancillary qubits" used as extra working space) performing the mapping* P*. That is for all* $|\Phi\rangle$*, the fixed sequenceS performs* :

$$|\Phi\rangle \otimes |\rho\rangle \xrightarrow{S} |\Psi\rangle \tag{18}$$

where the mapping is a composition of linear operators, so that is linear operator also, in the view that quantum mechanics has linear evolution, so that quantum computer cannot solve NP-complete problems in polynomial time. The definition above just mean that quantum mechanics allows only two methods to change the state of a system :

1. **Unitary transformation** : any state change of an isolated system must be reversible, and must satisfy $\sum_i |\alpha_i|^2 = 1$ where the α_i are the probability amplitudes associated to the ith orthonormal basis element $|i\rangle$, which combined leads to unitary operations U on the state : a state $|\Phi\rangle$ can only be transformed to a state $U(|\Phi\rangle)$ by the unitary matrix U where $UU^\dagger = I$
2. **Measurement operator** : when applying a measurement to a quantum state returns a value with a probability related to the quantum states amplitude coefficients and places the system into the state whose value was returned. Quantum measurement are mathematically a collection of measurements operators $\{M_m\}$ that preserve probability : $\sum_m M_m^\dagger M_m = I$
3. **Combining state** : quantum mechanics allow to concatenate two quantum register on n and m qubits with states $|\Phi\rangle$ and $|\Psi\rangle$ respectively, using the tensor product state $|\Phi\rangle \otimes |\Psi\rangle$ in complex 2^{n+m} dimensional space.

3.3.2 Proof intuition

For the complete (*and beautiful*) proof, we refer the reader to [2]. But for the sake of completeness we just give some intuitive insights of how it is done.

1. First he show that the componentwise multiplication step of the convolution algorithm (*step 4* of the *Algorithm 1* described above) has no quantum counterpart, it does so by :
   — Studying requirements on a linear transformation (unitary transforms and measurement systems are linear operators) that attempts this step.
   — Then he show that there is no physically realizable process P that only consist of unitary transformation, measurements operator and combination of states that can perform this step.
   — This prove that componentwise multiplication step in not computable on a quantum computer.
2. Then he show that any physical process able to compute the quantum convolution problem must be able to compute the impossible componentwise multiplication step, then we reach a contradiction.
3. Quantum convolution cannot be done on quantum state.

Thus the replacement of the convolution algorithm in the quantum world cannot be achieved in a*direct*, simple manner, but must be approach using more sophisticated procedure, avoiding the impossible componentwise multiplication step.

3.4 Quantum Algorithm for Image Filtering

Therefore replacing the convolution algorithm in the quantum world cannot be achieved in a*direct* way. As Lomont notice this is only and directly related to mathematical definition of the convolution operator but not to the image processing task that it is usually used to perform. Thus the Lomont proof states that the convolution algorithm is not physically realizable on a quantum computer but makes no claims about *filtering a signal on a quantum computer*. Indeed [1] have shown that it could be approach by more sophisticated techniques.
Caraiman and Manta have shown in [1] that in order to derive to convolution step of the filtering algorithm one can take as a *quantum Oracle* the function that filter the desired (*good)* frequencies from the undesired (*bad*) ones without actually *transforming* the register into a filtered version of the input image but rather into a superposition of two image : one containing the good frequencies and one containing the bad frequencies. It follows that their quantum filtering algorithm outputs the input image itself in a frequency segmented manner and do not output a convolved version of it. Indeed what the Lomont proof states is that a quantum register containing the quantum image and the quantum filter cannot be ***transformed*** in the convolution of both.

3.4.1 Algorithm Analysis

In order to distinguish between the two images $|I_{good}\rangle$ containing the desired frequency components and $|I_{bad}\rangle$ containing the undesired frequency components, they exploit the *quantum interference phenomenon*, using an additional qubit initialised in state $|0\rangle$ to reinterpret the image as a superposition of $|I_{good}\rangle$ and $|I_{bad}\rangle$. Therefore this additional qubit can be used to make distinction between the two images. Let's analyse the states of the quantum image filtering algorithm at each step of the computation.

1. First we need to prepare the input state $|I_0\rangle$, which consist of a tensor product state between the quantum input image and the additional qubit in state $|0\rangle$:

$$|I_0\rangle = |Q\rangle \otimes |0\rangle = \frac{1}{2^n} \sum_{y=0}^{2^n-1} \sum_{x=0}^{2^n-1} \sum_{j=0}^{2^m-1} \alpha_{xyj} |j\rangle |y\rangle |x\rangle |0\rangle \tag{19}$$

   where $|Q\rangle$ is the quantum register containing our quantum image as described in (1).

2. Then we apply the QFT on the initial state $|I_0\rangle$:

$$
\begin{aligned}
|I_1\rangle &= (I_m \otimes QFT_{2^{2n}})\,|Q\rangle \otimes I\,|0\rangle && (20)\\
&= \frac{1}{2^n}\sum_{y=0}^{2^n-1}\sum_{x=0}^{2^n-1}\sum_{j=0}^{2^m-1}\alpha_{xyj}\,|j\rangle\, QFT_{2^{2n}}(|y\rangle\,|x\rangle)\,|0\rangle && (21)\\
&= \frac{1}{2^n}\sum_{y=0}^{2^n-1}\sum_{x=0}^{2^n-1}\sum_{j=0}^{2^m-1}\alpha_{xyj}\,|j\rangle\,(QFT_{2^n}\,|y\rangle)(QFT_{2^n}\,|x\rangle)\,|0\rangle && (22)\\
&= \frac{1}{2^n}\sum_{y=0}^{2^n-1}\sum_{x=0}^{2^n-1}\sum_{j=0}^{2^m-1}\alpha_{xyj}\,|j\rangle\left[\frac{1}{\sqrt{2^n}}\sum_{k=0}^{2^n-1}e^{\frac{2i\pi yk}{2^n}}\,|k\rangle\,\frac{1}{\sqrt{2^n}}\sum_{l=0}^{2^n-1}e^{\frac{2i\pi xl}{2^n}}\,|l\rangle\right]|0\rangle && (23)\\
&= \frac{1}{2^{2n}}\sum_{y=0}^{2^n-1}\sum_{x=0}^{2^n-1}\sum_{j=0}^{2^m-1}\sum_{k,l=0}^{2^n-1}\alpha_{xyj}e^{\frac{2i\pi yk}{2^n}}e^{\frac{2i\pi xl}{2^n}}\,|j\rangle\,|k\rangle]\,|l\rangle\,|0\rangle && (24)\\
&= \frac{1}{2^{2n}}\sum_{y=0}^{2^n-1}\sum_{x=0}^{2^n-1}\sum_{j=0}^{2^m-1}\sum_{k,l=0}^{2^n-1}\alpha_{xyj}\; e^{\frac{2i\pi(yk+xl)}{2^n}}\,|j\rangle\,|k\rangle\,|l\rangle\,|0\rangle && (25)
\end{aligned}
$$

where I_m and I denote here the identity operator on m and 1 qubit respectively. In the above calculation one can use the fact that the QFT on k qubit is similar to the k-fold tensor product of k one qubit QFT :

$$
QFT_{2^k}\,|i\rangle_k = QFT^{\otimes k}\,|i_{k-1}\dots i_0\rangle = QFT\,|i_{k-1}\rangle \otimes \cdots \otimes QFT\,|i_0\rangle \qquad (26)
$$

and also the *phase kick back effect* which is a consequence of the following tensor product property :

$$
(\lambda A) \otimes B = \lambda(A \otimes B) = A \otimes (\lambda B) \qquad (27)
$$

meaning that the phase is conserved through tensor product, so it doesn't matter in which register the phase appears.

The QFT targets information about both color and position, indeed it as a form $I \otimes U$, where U is a n qubits unitary operator, I is the identity operator. The application of QFT on quantum image can be consider as the application of Fourier Transform on the α part of the quantum image state coefficients, when applied to a superposition of state $|l\rangle$ with complex amplitude α it outputs another superposition of states $|k\rangle$ with amplitude β_k related to α as in the following calculation :

$$
\begin{aligned}
|I_{QFT}\rangle &= \frac{1}{2^n}\sum_{l=0}^{2^{2n}-1}\sum_{j=0}^{2^m-1}\alpha_{lj}\,|j\rangle \otimes QFT(|l\rangle) && (28)\\
&= \frac{1}{2^n}\sum_{k=0}^{2^{2n}-1}\sum_{j=0}^{2^m-1}\beta_k\,|jk\rangle && (29)
\end{aligned}
$$

where :

$$\beta_k = \frac{1}{2^n} \sum_{l=0}^{2^{2n}-1} e^{2i\pi lk/2^{2n}} \alpha l j \tag{30}$$

At this point we have the quantum state $|I_1\rangle$ containing the spectrum (frequency domain representation) of our input image, and thus can be already thought (thanks to linearity) as a superposition of a state containing the frequencies that will pass through the filter and a state containing the frequencies that will be discarded by the filter. Let's call $|I_{1\ good}\rangle$ and $|I_{1\ bad}\rangle$ such states, and let g be the number of *good* frequencies, $|I_1\rangle$ can be represented as :

$$|I_1\rangle = \sqrt{\frac{g}{2^{2n}}}\,|I_{1\ good}\rangle + \sqrt{\frac{2^{2n}-g}{2^{2n}}}\,|I_{1\ bad}\rangle \tag{31}$$

3. The next step is the *critical one*, the analogue of the convolution, meaning the filtering step. At this point the autors of [1] build a quantum Oracle U_H using the desired *filter function* $H(k,l)$.
   A quantum Oracle is a quantum circuit that *recognizes* solution to a given problem, and is supplied as a black box that can provides *yes-no* binary answers to a specific question, which in our case is : *does this frequency belong to this specific frequency set ?*
   They show that the additional qubit ($|0\rangle$) can be use to distinguish between the two desired state when applying the Oracle on the $|I_1\rangle$ state, where the the Oracle U_H and the filter function $H(k,l)$ are respectively defined as :

$$|k\ l\rangle\,|z\rangle \xrightarrow{U_H} |k\ l\rangle\,|z \oplus H(k,l)\rangle \tag{32}$$

$$H(k,l) = \begin{cases} 1 & \text{if } k,l \in S_{good} \\ 0 & \text{if } k,l \in S_{bad} \end{cases} \tag{33}$$

   where S_{good} and S_{bad} are respectively the set of coordinates for the *good* and *bad* frequencies classified according to the desired filter function, and where $|z\rangle$ in our case is the $|0\rangle$ computational basis state. Now using the so-called Oracle, one can compute the filtering step as follows :

$$
\begin{aligned}
|I_2\rangle &= (I_m \otimes U_H)\,|I_1\rangle & (34)\\
&= \frac{1}{2^{2n}} \sum_{y=0}^{2^n-1}\sum_{x=0}^{2^n-1}\sum_{j=0}^{2^m-1}\sum_{k,l=0}^{2^n-1} \alpha_{yxj}\; e^{\frac{2i\pi(yk+xl)}{2^n}}\;|j\rangle\, U_H(|k\rangle\,|l\rangle\,|0\rangle) & (35)\\
&= \frac{1}{2^{2n}} \sum_{y=0}^{2^n-1}\sum_{x=0}^{2^n-1}\sum_{j=0}^{2^m-1}\sum_{k,l\in S_{good}} \alpha_{yxj}\; e^{\frac{2i\pi(yk+xl)}{2^n}}\;|j\rangle\,|k\rangle\,|l\rangle\,|1\rangle \\
&+ \frac{1}{2^{2n}} \sum_{y=0}^{2^n-1}\sum_{x=0}^{2^n-1}\sum_{j=0}^{2^m-1}\sum_{k,l\in S_{bad}} \alpha_{yxj}\; e^{\frac{2i\pi(yk+xl)}{2^n}}\;|j\rangle\,|k\rangle\,|l\rangle\,|0\rangle & (36)
\end{aligned}
$$

From the equation (20) we see that the Oracle only acts on the position (spatial frequencies) qubits and leaves the colors qubits and corresponding amplitudes unaffected by its action.
At this point one can build the commonly used ideal filter functions by the means of the corresponding S_{good} and S_{bad} as summarized in the following table :

Filter	**Frequency Sets**
Low-pass	$\begin{cases} S_{good} = \{k,l \mid D(k,l) \leq D_{cutoff}\} \\ S_{bad} = \{k,l \mid D(k,l) > D_{cutoff}\} \end{cases}$
High-pass	$\begin{cases} S_{good} = \{k,l \mid D(k,l) \geq D_{cutoff}\} \\ S_{bad} = \{k,l \mid D(k,l) < D_{cutoff}\} \end{cases}$
Band-pass	$\begin{cases} S_{good} = \{k,l \mid D_L \leq D(k,l) \leq D_H\} \\ S_{bad} = \{k,l \mid D(k,l) < D_L \cap D(k,l) > D_H\} \end{cases}$
Band-stop	$\begin{cases} S_{good} = \{k,l \mid D(k,l) < D_L \cap D(k,l) > D_H\} \\ S_{bad} = \{k,l \mid D_L \leq D(k,l) \leq D_H\} \end{cases}$

TABLE 1 – Table of some ideal filter and their corresponding Frequency Sets used by the Oracle U_H

4. Once the quantum image spectrum has been separated into *desired* frequency sets, one can perform the QFT^{-1} that will transform the spectrum of the two images into theirs spatial representations. For notation convenience let's introduce $\tilde{\alpha}_{yxj} = \alpha_{yxj}\; e^{\frac{2i\pi(yk+xl)}{2^n}}$. As shown in [1] the outputs of the QFT^{-1} step can be considered as a superposition of two image, for example in the case where the Oracle is build using the frequency sets associated with an ideal low pass filter function, one will

get a superposition of one image constructed with the low frequency component of the image (global shapes and forms), with another one constructed with the high frequency component (details and edges). The following calculation shows how such images could be derived :

$$|I_3\rangle = \tag{37}$$

$$= \frac{1}{2^{2n}} \sum_{y=0}^{2^n-1} \sum_{x=0}^{2^n-1} \sum_{j=0}^{2^m-1} \sum_{k,l \in S_{good}} \tilde{\alpha}_{yxj} |j\rangle\, QFT_{2^n}^{-1}(|k\rangle\,|l\rangle)\,|1\rangle$$
$$+ \frac{1}{2^{2n}} \sum_{y=0}^{2^n-1} \sum_{x=0}^{2^n-1} \sum_{j=0}^{2^m-1} \sum_{k,l \in S_{bad}} \tilde{\alpha}_{yxj} |j\rangle\, QFT_{2^n}^{-1}(|k\rangle\,|l\rangle)\,|0\rangle \tag{38}$$

$$= \frac{1}{2^{2n}} \sum_{y=0}^{2^n-1} \sum_{x=0}^{2^n-1} \sum_{j=0}^{2^m-1} \sum_{k,l \in S_{good}} \tilde{\alpha}_{yxj} |j\rangle\, QFT_{2^n}^{-1}(|k\rangle) QFT_{2^n}^{-1}(|l\rangle)\,|1\rangle$$
$$+ \frac{1}{2^{2n}} \sum_{y=0}^{2^n-1} \sum_{x=0}^{2^n-1} \sum_{j=0}^{2^m-1} \sum_{k,l \in S_{bad}} \tilde{\alpha}_{yxj} |j\rangle\, QFT_{2^n}^{-1}(|k\rangle) QFT_{2^n}^{-1}(|l\rangle)\,|0\rangle \tag{39}$$

$$= \frac{1}{2^{2n}} \sum_{y=0}^{2^n-1} \sum_{x=0}^{2^n-1} \sum_{j=0}^{2^m-1} \sum_{k,l \in S_{good}} \tilde{\alpha}_{yxj} |j\rangle\, \frac{1}{2^n} \left[\sum_{c=0}^{2^n-1} e^{\frac{-2i\pi kc}{2^n}} |c\rangle \sum_{r=0}^{2^n-1} e^{\frac{2i\pi lr}{2^n}} |r\rangle \right] |1\rangle$$
$$+ \frac{1}{2^{2n}} \sum_{y=0}^{2^n-1} \sum_{x=0}^{2^n-1} \sum_{j=0}^{2^m-1} \sum_{k,l \in S_{bad}} \tilde{\alpha}_{yxj} |j\rangle\, \frac{1}{2^n} \left[\sum_{c=0}^{2^n-1} e^{\frac{-2i\pi kc}{2^n}} |c\rangle \sum_{r=0}^{2^n-1} e^{\frac{2i\pi lr}{2^n}} |r\rangle \right] |0\rangle \tag{40}$$

$$= \frac{1}{2^{3n}} \sum_{c=0}^{2^n-1} \sum_{r=0}^{2^n-1} \sum_{j=0}^{2^m-1} \sum_{k,l \in S_{good}} \sum_{y=0}^{2^n-1} \sum_{x=0}^{2^n-1} \tilde{\alpha}_{yxj} e^{\frac{-2i\pi(kc+lr)}{2^n}} |j\rangle\,|c\rangle\,|r\rangle\,|1\rangle$$
$$+ \frac{1}{2^{3n}} \sum_{c=0}^{2^n-1} \sum_{r=0}^{2^n-1} \sum_{j=0}^{2^m-1} \sum_{k,l \in S_{bad}} \sum_{y=0}^{2^n-1} \sum_{x=0}^{2^n-1} \tilde{\alpha}_{yxj} e^{\frac{-2i\pi(kc+lr)}{2^n}} |j\rangle\,|c\rangle\,|r\rangle\,|0\rangle \tag{41}$$

$$\tag{42}$$

here one can notice that :

$$|I_3\rangle = \tag{43}$$

$$= \frac{1}{2^{3n}} \sum_{c=0}^{2^n-1} \sum_{r=0}^{2^n-1} \sum_{j=0}^{2^m-1} \sum_{k,l \in S_{good}} \sum_{y=0}^{2^n-1} \sum_{x=0}^{2^n-1} \alpha_{yxj} e^{\frac{2i\pi(yk+xl)}{2^n}} e^{\frac{-2i\pi(kc+lr)}{2^n}} |j\rangle |c\rangle |r\rangle |1\rangle$$

$$+ \frac{1}{2^{3n}} \sum_{c=0}^{2^n-1} \sum_{r=0}^{2^n-1} \sum_{j=0}^{2^m-1} \sum_{k,l \in S_{bad}} \sum_{y=0}^{2^n-1} \sum_{x=0}^{2^n-1} \alpha_{yxj} e^{\frac{2i\pi(yk+xl)}{2^n}} e^{\frac{-2i\pi(kc+lr)}{2^n}} |j\rangle |c\rangle |r\rangle |0\rangle \tag{44}$$

$$= \frac{1}{2^n} \sum_{c=0}^{2^n-1} \sum_{r=0}^{2^n-1} \sum_{j=0}^{2^m-1} \frac{1}{2^{2n}} \left[\alpha_{yxj} \sum_{k,l \in S_{good}} \sum_{y=0}^{2^n-1} e^{\frac{2i\pi k(y-c)}{2^n}} \sum_{x=0}^{2^n-1} e^{\frac{2i\pi l(x-r)}{2^n}} \right] |j\rangle |c\rangle |r\rangle |1\rangle$$

$$+ \frac{1}{2^n} \sum_{c=0}^{2^n-1} \sum_{r=0}^{2^n-1} \sum_{j=0}^{2^m-1} \frac{1}{2^{2n}} \left[\alpha_{yxj} \sum_{k,l \in S_{bad}} \sum_{y=0}^{2^n-1} e^{\frac{2i\pi k(y-c)}{2^n}} \sum_{x=0}^{2^n-1} e^{\frac{2i\pi l(x-r)}{2^n}} \right] |j\rangle |c\rangle |r\rangle |0\rangle \tag{45}$$

$$= \frac{1}{2^n} \sum_{c=0}^{2^n-1} \sum_{r=0}^{2^n-1} \frac{1}{2^{2n}} \sum_{j=0}^{2^m-1} \alpha^g_{rcj} |j\rangle |c\rangle |r\rangle |1\rangle$$
$$+ \frac{1}{2^n} \sum_{c=0}^{2^n-1} \sum_{r=0}^{2^n-1} \frac{1}{2^{2n}} \sum_{j=0}^{2^m-1} \alpha^b_{rcj} |j\rangle |c\rangle |r\rangle |0\rangle \tag{46}$$

where the complex terms in $[\ldots]$ is nothing more than the amplitude associated with state $|j\rangle$, in other word the superposition $\frac{1}{2^{2n}} \sum_{j=0}^{2^m} \alpha^g_{rtj} |j\rangle$ is the color associated with the pixel at position $|rt\rangle$ in the filtered image constructed with the proper frequencies, same thing with $\frac{1}{2^{2n}} \sum_{j=0}^{2^m} \alpha^b_{rtj} |j\rangle$. Thus the probability that a measurement results in outcome j is :

$$P^g_j = \left| \frac{1}{2^{2n}} \sum_{y=0}^{2^n-1} \sum_{x=0}^{2^n-1} \sum_{k,l \in S_{good}} \alpha_{yxj} e^{\frac{2i\pi k(y-c)}{2^n}} e^{\frac{2i\pi l(x-r)}{2^n}} \right|^2 \text{ for } c, r \in [0, 2^n - 1] \tag{47}$$

$$P^b_j = \left| \frac{1}{2^{2n}} \sum_{y=0}^{2^n-1} \sum_{x=0}^{2^n-1} \sum_{k,l \in S_{bad}} \alpha_{yxj} e^{\frac{2i\pi k(y-c)}{2^n}} e^{\frac{2i\pi l(x-r)}{2^n}} \right|^2 \text{ for } c, r \in [0, 2^n - 1] \tag{48}$$

from there one can easily verified that the α^g_{rtj} and α^b_{rtj} and indeed proper normalized quantum amplitudes, meaning that $\sum_j |\alpha^g_{rtj} + \alpha^b_{rtj}|^2 = 1$, let's sum the S_{good} and S_{bad} frequency sets over all k, l to see how the sum of the *good* and *bad*quantum amplitudes behaves :

$$P_j^{tot} = \sum_{j=0}^{2^n-1} \left| \frac{1}{2^{2n}} \sum_{y=0}^{2^n-1} \sum_{x=0}^{2^n-1} \sum_{k,l}^{2^n-1} \alpha_{yxj} e^{\frac{2i\pi k(y-c)}{2^n}} e^{\frac{2i\pi l(x-r)}{2^n}} \right|^2 \text{ for } c,r \in [0, 2^n-1] \tag{49}$$

$$= \sum_{j=0}^{2^n-1} \left| \frac{1}{2^{2n}} \sum_{y=0}^{2^n-1} \sum_{x=0}^{2^n-1} \alpha_{yxj} \sum_{k=0}^{2^n-1} \left(e^{\frac{2i\pi(y-c)}{2^n}} \right)^k \sum_{l=0}^{2^n-1} \left(e^{\frac{2i\pi(x-r)}{2^n}} \right)^l \right|^2 \text{ for } c,r \in [0, 2^n-1] \tag{50}$$

using the geometric series sum form, one can notice that :

$$\sum_{k=0}^{2^n-1} \left(e^{\frac{2i\pi(y-c)}{2^n}} \right)^k = \begin{cases} \dfrac{1-e^{2i\pi(y-c)}}{1-e^{\frac{2i\pi(y-c)}{2^n}}} & \text{if } y \neq c \\ \sum_{k=0}^{2^n-1} e^0 = 2^n & \text{if } y = c \end{cases} \tag{51}$$

since the exact same reasoning can be done for x and r, we are left with :

$$P_j^{tot} = \sum_{j=0}^{2^n-1} \left| \frac{1}{2^{2n}} \alpha_{yxj} 2^n 2^n \right|^2 \text{ for } y = r \text{ , } x = c \text{ and } c,r \in [0, 2^n-1] \tag{52}$$

$$= \sum_{j=0}^{2^n-1} |\alpha_{rcj}|^2 \tag{53}$$

$$= 1 \tag{54}$$

since $\alpha_{rcj} = 1$ by construction for a given pixel with position r, c with color j and 0 otherwise.

From (34) one can recognize that the two sum terms have a quantum image form, where $|r\rangle$ and $|c\rangle$ register encode the *row* and *column* coordinates of a pixel, respectively, and as usual the m qubits of $|j\rangle$ are used in a superposition manner to encode the color of all the pixels, thus one can rewrite (34) as an explicit superposition of two images, meaning :

$$|I_3\rangle = |Q_{good}\rangle \otimes |1\rangle + |Q_{bad}\rangle \otimes |0\rangle \tag{55}$$

where $|Q\rangle = |C\rangle_m \otimes |P\rangle_{2n}$ is the form of a quantum image register as firstly constructed by Caraiman and Manta in [4]. This is the main advantage of using an Oracle instead of trying to *directly* implement the quantum analogue of the convolution procedure that obviously try to *transform* the register, here instead the whole spatial frequency set of the quantum image is still present in the algorithm output, but in distinguishable states. Thus further processing steps could then be applied to either of the two quantum images in the final quantum superposition by making use of controlled operators on the oracle qubits to manipulate one image or the other.

4 Extract information from the filtered images

4.1 Retrieval of the whole image

Finally, once the filtering is done (which is often just a pre-processing step embedded as a building block in a more large procedure) one might hope to extract some useful informations from the filtered image by just "*looking*" at it. Unfortunately this is not directly achievable since in our case the images are store in quantum states, meaning that if a measurement is performed on the final state $|I_3\rangle$, it will just samples from the images and reveals the color at a single pixel position. Moreover, the state of the measured quantum register storing the images superposition will *collapse* during the measurement to one of its basis states, therefore measuring the state again after the first measurement was performed will yields the exact same state as the initial measurements with unit probability.

Thus, retrieving the whole image(s) from a quantum superposition state requires, first that multiple instances of the input image are prepared - no matter what quantum image representation we used (first or second class from *part 2.*) - then the quantum filtering algorithm must be run on each of the image instances, and finally one has to samples each output images until all the colors of all the pixels positions are sampled.
Despite this sampling issue, we have seen that the computational advantage of the quantum image encoding we used (2.1) initially proposed by the authors in [4]) is that that both color and position of a pixel can be retrieved deterministically through a finite number of projective measurement.
However the deterministic retrieval of the of pixel colors by projective measurements is only possible as long as the α_{ij} remains binary coefficient under the action of our algorithm, this is *no more the case* after we applied the quantum filtering algorithm since the amplitude of our two images are then real values, and thus requires here also a statistical procedure (as in 2.1) to be be retrieved.
There are different approachs to perform this statistical procedure according to quantum sampling theory to estimate the quantum probability amplitudes of the quantum states encoding the colors of each pixels within a given accuracy. Even if those are beyond the scope of this report, for the sake of completeness, we can cite the *Quantum storage and retrieval protocol* proposed by Venegas-Andraca and Bose in [7]. As stated before this protocol requires to deal with several instances of the input image, apply the same algorithm to all of them and then sample using measurement operators. The multi-sampling behaviour

of this kind of procedure try to minimize the uncertainty in the retrieval of the quantum parameter. This uncertainty is inherent to the postulates of quantum mechanics about the retrieval of a quantum stated above about the estimation of a quantum amplitude through a finite number of quantum measurements.

4.2 Process some additional quantum algorithms

There exists also other alternatives for gaining some useful insights from a quantum-transformed image, instead of retrieving the whole classical image to infer classical computing information from the quantum image, and since in our setting the filtering procedure is often a pre-processing step, one can instead perform some more processing steps on the quantum register(s) storing the image(s), and hence other classes of measurements could reveal some useful properties of the processed image without the need to actually "*look*" at it entirely.
For example, in our case, the *segmentation* of the high frequency image can yield a quantum register containing only the pixel belonging to the edges of an object represented in the image. Following the same reasoning other transformations/segmentations of any given frequency-band can yield to quantum register containing only the pixel belonging to some spatial useful information encoded by this specific frequency band.

Furthermore, statistical information about the shapes (perimeter, area, spatial descriptors, etc.) of the objects represented in the image could be accurately obtained using several variations of *Groover quantum search, quantum counting or quantum intergal estimation*, those informations cold then be determined by measuring the output state of these operators and thus there is no need to retrieve the whole classical image from the quantum one. This are left for future quantum algorithm development but it is sound that this kind of statistical informations could be used for image classification for quantum machine learning, meaning comparing images based on this kind of statistical descriptors in a recognition quantum computer vision system. And since both *QFT* and *Quantum Search* provide speed up compared to their classical analogue, implementing a content-based image retrieval system on a quantum computer will bring significant speed compared to actual classical system.

This is true for 1-D and 2-D signals (images), but as the quantum analogue of Fourier Transform and Filters have been proved to be implementable and very efficient on a quantum computer, one can reasonably expect that quantum counterpart of *Graph Fourier Transform / Graph Spectral Filter* and *Manifold Harmonic Transform / Manifold Spectral Filters* will certainly be developed in the future and hence yield to a variety of algorithms, applications and content-based learning systems for Graph/Manifold that will outperform in complexity the classical ones thanks to the qubit power !

5 Simulation

To demonstrate the soundness of their algorithm, the authors implement a simulation of the quantum filtering operation in *MATLAB* on 32x32 gray scale images by representing quantum image as α_{ij} matrices according to (4) ad by applying the quantum filtering operation (45) to compute the the intensity values of the pixels in the final quantum states that represent the filtered image $|Q_{good}\rangle$ and $|Q_{bad}\rangle$.

Three 32x32 images were used, a synthetic image containing only 2 gray levels, and two sub-image A and B from a microscopy image containing respectively 4 and 189 different gray levels. For each of these images the color information of each pixel were encoded using $m = 8$ qubits to encode 256 possible gray levels. The pixel positions were encoded using 10 qubits.

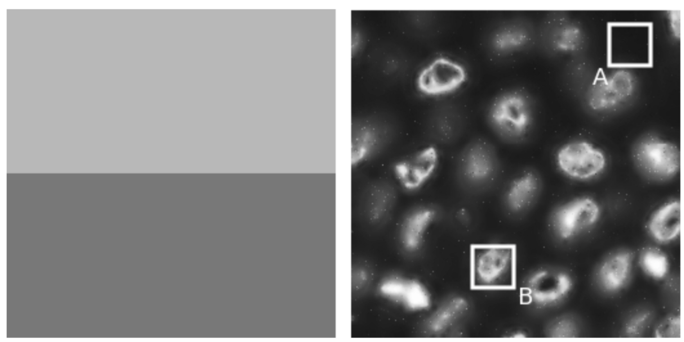

FIGURE 3 – Test images : Left - 32x32 synthetic image with two gray levels. Right - Microscopy image, where A and B are 32x32 sub-image used for the testing

The images were then filtered using an oracle build on an high-pass filter with cutoff frequency $D_0 = 0.2 \times 32 = 6.4$, the resulting high and low spatial frequencies - corresponding to $|Q_{good}\rangle$ and $|Q_{bad}\rangle$ states respectively - are shown in the figure below.

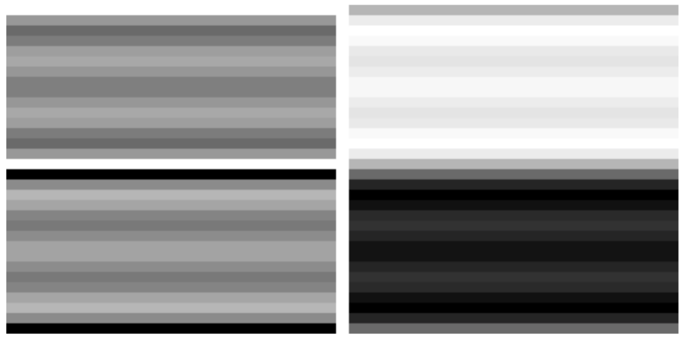

FIGURE 4 – Result of filtering the synthetic image with an high-pass filter with cutoff frequency $D_0 = 0.2 \times 32$. Left - High frequencies image. Right - Corresponding low frequencies image

As one could expect the high frequencies image contain information about edges and boundaries - it emphasizes the horizontal edge in the middle, while the low frequencies image has a smoothing (blurring) effect. The horizontal oscillating bands in the above filtered images are due to the well known ringing effect of spectral ideal filters.
The authors store for a given pixel coordinate $(3, 3)$ of the synthetic image, the gray levels and the corresponding quantum representation for the original image - high frequencies and low frequencies images :

	input image	high-freq. image ($\lvert Q_{good}\rangle$)	low-freq. image ($\lvert Q_{bad}\rangle$)
gray level	170	-3.91	173.91
$\lvert C\rangle_8$	$1\lvert 170\rangle$	$0.0559\lvert 100\rangle$ $-0.0559\lvert 170\rangle$	$-0.0559\lvert 100\rangle$ $+1.0559\lvert 170\rangle$

In the resulting filtered images, the intensity value of each pixel is, as we have shown, represented by a quantum superposition of the 2 basis states colors corresponding to the gray levels in the original image. Furthermore we can also observe that the amplitudes of the quantum states $|Q_{good}\rangle$ and $|Q_{bad}\rangle$, yield as expected to $\sum_j |\alpha^g_{rtj} + \alpha^b_{rtj}|^2 = 1$ and

moreover is equivalent to the quantum representation of the original image where there were filtered from, which is sound with one can expect from the classical setting where the two frequency filtered image sum to the original image.
The authors choose for displaying purposes to extract the classical representation of the high and low frequencies image from the quantum superposition by multiplying the amplitudes with the integer encoding of the state vector and as in the classical filtering setting some negative gray level values may be obtained, and similarly as in the classical case we just rescale the so-obtained coefficient according to the minimum value (0 -black) and maximum value (255 - white). For instance the gray level of the $(3,3)$ pixel in the $|Q_{good}\rangle$ (high-freq image) was map to $-3.91 \xrightarrow{rescale} 105^{th}$ gray level while in the $|Q_{good}\rangle$ (low-freq image) it was map to $173.91 \xrightarrow{rescale} 246^{th}$ gray level.

For the sub-image A and B, the very same procedure was used, we will focus on sub-image B since it is the more interesting.

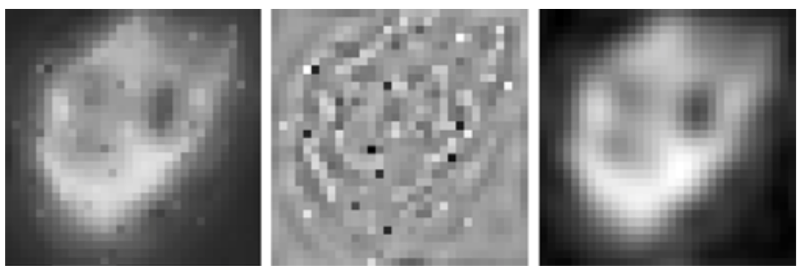

FIGURE 5 – Result of filtering the sub-image B with an high-pass filter with cutoff frequency $D_0 = 0.2 \times 32$. Left - Original image. Center - High frequencies image. Right - Corresponding low frequencies image

Same observation here, the high frequencies image contain information about edges and boundaries of the object, while the low frequencies image has a smoothing effect and present the global shape of the object.
Since the original sub-image B contains 189 gray levels, the quantum representation of each pixel in the above filtered images is described as a quantum superposition of 189 basis vectors corresponding to the gray levels used in the original image. The quantum amplitudes of the superposition representing the intensity value of the $(3,3)$ pixel in the the $|Q_{good}\rangle$ of sub-image B are plotted in the below figure.

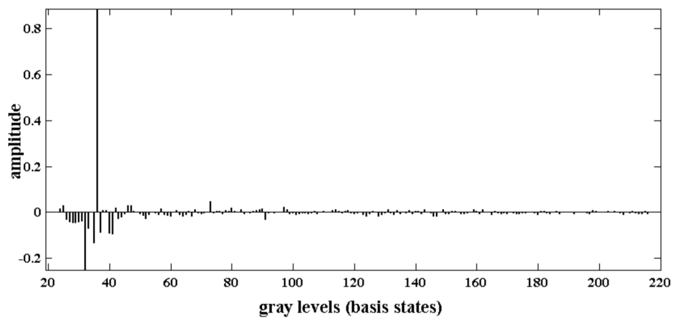

FIGURE 6 – Quantum representation of the pixel with coordinates (3,3) in sub-image B filtered by an high-pass filter of cutoff frequency $D_0 = 0.2 \times 32 = 6.4$. The gray level of the pixel turns out to be 0.2788 and is expressed as a superposition of the quantum states representing all the gray level presents in the original image

6 Conclusion

We saw that despite the speed up introduces by the quantum analogue of the Fourier transform, the quantum implementation of the filtering operation in the frequency domain cannont be achieved in a straightforward way because the quantum convolution of two sequences encoded in quantum states is not physically possible. The authors proposed a workaround based on the use of a quantum oracle that implement the filer function. The tricks avoiding the impossible convolution was to interpret the image as a superposition of the two filtered images containing respectively *good* and *bad* frequencies according to the filter oracle classification. Doing so one does not have to convolve the image with a filter but instead use the filter to distinguish between the two filtered images.

The main complexity advantage of this quantum algorithm compare to its classical counter part (FFT) is the exponential speed provide by the QFT. Although this exponential speed up is usually hard to exploit because the set of Fourier coefficients are store as probability amplitudes of quantum states and thus cannot be directly accessed, in this filtering algorithm the exponential speed up of the QFT is preserved since one does not have to extract this set of Fourier coefficients in order to obtain the filtered images.

On other advantages of implementing such algorithm on a quantum computer is related to the reversibility of the allowed quantum computations, meaning that unlike in the classical

setting, one can reconstruct the original image out of the filtered ones.
In contrary the main disadvantages of this quantum translation is that the retrieval of the filtered images is not straightforward unlike in the classical case, because one again informations are encoded in the amplitudes of quantum states and cannot be accessed directly. But as we discussed in section 4.2, the retrieval might not be necessary since the filtering operation is often just a pre-processing step embedded as a building block in more complex procedure, so more computational steps could be applied without the need to actually retrieve the whole image by the means of controlled operation on the oracle qubits to further process either of the two filtered images.

Also unlike in the classical case, a considerable improvement of encoding image on a quantum computer is that the same m qubits are used to store the color of all the pixels in the image, hence only $m = 2^n$ qubits are needed to store a 2^nx2^n image composed of L gray levels, that is an an overall ***exponentially*** lower memory space usage compared to the classical case where $m2^{2n}$ bits are necessary to store the same image.

Références

[1] S.Caraiman, V.Manta, Quantum Image Filtering in the Frequency Domain, Advances in Electrocal and Computer Engineering 13-3, 2013.

[2] C.Lomont, Quantum Convolution and Quantum Correlation algorithms are physically impossible, Mathematics Subject Classification, 2003.

[3] J.Watrous, Lecture 9 : Phase Estimation (continued) ; the quantum Fourier transform, CPSC 519/618 : Quantum Computation, 2006.

[4] S.Caraiman, V.Manta, Image processing using quantum computing. System Theory, Control and Computing (ICSTCC), 1-6, 2012.

[5] S.Caraiman, V.Manta, Image Segmentation on a quantum computer. Quantum Inf Process. Springer, 2015

[6] P. Le, F. Dong, K. Hirota, A flexible representation of quantum images for polynomial preparation, image compression, and processing operations, Quantum Inf Process, vol. 10, 63-84, 2011

[7] S. Venegas-Andraca, S. Bose. Stroring, processing and retrieving an image using quantum mechanis. Proceedings of the SPIE 2003 Conference on uantum Information and Computation ; 137-147, 2003.